Scilight

Hydrology and Water Resources
https://www.sciltp.com/journals/hwr

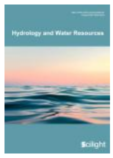

Review

Spatiotemporal Dynamics and Driving Mechanisms of Ecohydrological Cycles in Global Drylands: A Review Based on Multi-Source Remote Sensing

Jiawei Xie [1,2,3], Fei Gao [1,2,3,*], Laozi Jili [1,2,3], Jing Zhang [1,2,3], Shikun Sun [1,2,4], Fan Gao [5], Xiaotao Hu [1,2,3] and Pingan Jiang [6]

[1] Key Laboratory of Agricultural Soil and Water Engineering in Arid and Semiarid Areas, Ministry of Education, Northwest A&F University, Yangling 712100, China
[2] Institute of Water Saving Agriculture in Arid Regions of China, Northwest A&F University, Yangling 712100, China
[3] College of Water Resources and Architectural Engineering, Northwest A&F University, Yangling 712100, China
[4] Xinjiang Research Institute of Agriculture in Arid Areas, Urumqi 830052, China
[5] College of Hydraulic and Civil Engineering, Xinjiang Agricultural University, Urumqi 830052, China
[6] College of Resources and Environment, Xinjiang Agricultural University, Urumqi 830052, China
* Correspondence: gao.fei@nwafu.edu.cn

How To Cite: Xie, J.; Gao, F.; Jili, L.; et al. Spatiotemporal Dynamics and Driving Mechanisms of Ecohydrological Cycles in Global Drylands: A Review Based on Multi-Source Remote Sensing. *Hydrology and Water Resources* **2025**, *1*(1), 3. https://doi.org/10.53941/hwr.2026.100003.

Received: 28 August 2025
Revised: 1 October 2025
Accepted: 17 October 2025
Published: 3 November 2025

Abstract: Drylands, including hyper-arid, arid, and semi-arid regions, are critical components of the global ecosystem, and their hydrological cycles are highly sensitive to climate change. In this review, we compared widely used remote sensing products and integrated multi-source datasets to examine the spatiotemporal patterns of key hydrological variables between 2001 and 2022. We focused on precipitation, evapotranspiration, soil moisture, groundwater, and terrestrial water storage in drylands, and analyzed their driving mechanisms. During the study period, global precipitation increased significantly at 0.62 mm yr^{-1}, whereas precipitation in drylands declined and the extent of drylands expanded. Evapotranspiration rose at 2.26 mm yr^{-1}, with higher values concentrated in drylands. Soil moisture exhibited a significant decreasing trend of 0.20 mm yr^{-1}, particularly in arid and semi-arid regions, indicating intensified surface dryness and reduced soil water availability. Groundwater storage decreased markedly at 2.18 mm yr^{-1}, with severe depletion in several dryland basins. Terrestrial water storage also declined at 3.16 mm yr^{-1}, with widespread negative anomalies across drylands. Correlation analyses indicated general positive associations between NDVI and precipitation and terrestrial water storage, and negative associations with evapotranspiration. The spatiotemporal evolution of hydrological processes in drylands was jointly driven by climate change, natural variability, and human activities: global warming intensifies atmospheric evaporative demand and alters circulation patterns, large-scale oscillations modulate precipitation variability, and human interventions reshape the spatial and temporal distribution of water resources. This review provides a comprehensive synthesis of multi-source remote sensing datasets to quantify hydrological changes and their ecological implications in global drylands, offering new insights into the mechanisms of water scarcity and vegetation responses under climate change.

Keywords: drylands; hydrological cycle; remote sensing; spatiotemporal dynamics

1. Introduction

Drylands, as essential components of the global ecosystem, are highly sensitive to climate change. According to the United Nations Environment Programme [1], drylands encompass hyper-arid, arid, and semi-arid regions. Based on the aridity index (AI, the ratio of mean annual precipitation (P) to mean annual potential evapotranspiration (PET)), the global land surface can be classified into hyper-arid, arid, semi-arid, sub-humid, and humid zones (Figure 1a) [2], with drylands accounting for approximately 40% of the terrestrial area. Due to evapotranspiration in drylands generally exceeds precipitation and only 7.7% of the world's renewable surface water is available there, these regions are characterized by weak soil moisture storage capacity and sparse vegetation (Figure 1b), making them highly prone to desertification and ecological degradation. Understanding the spatiotemporal dynamics and driving mechanisms of hydrological processes in drylands is therefore crucial for clarifying global water resource patterns and ensuring ecological security.

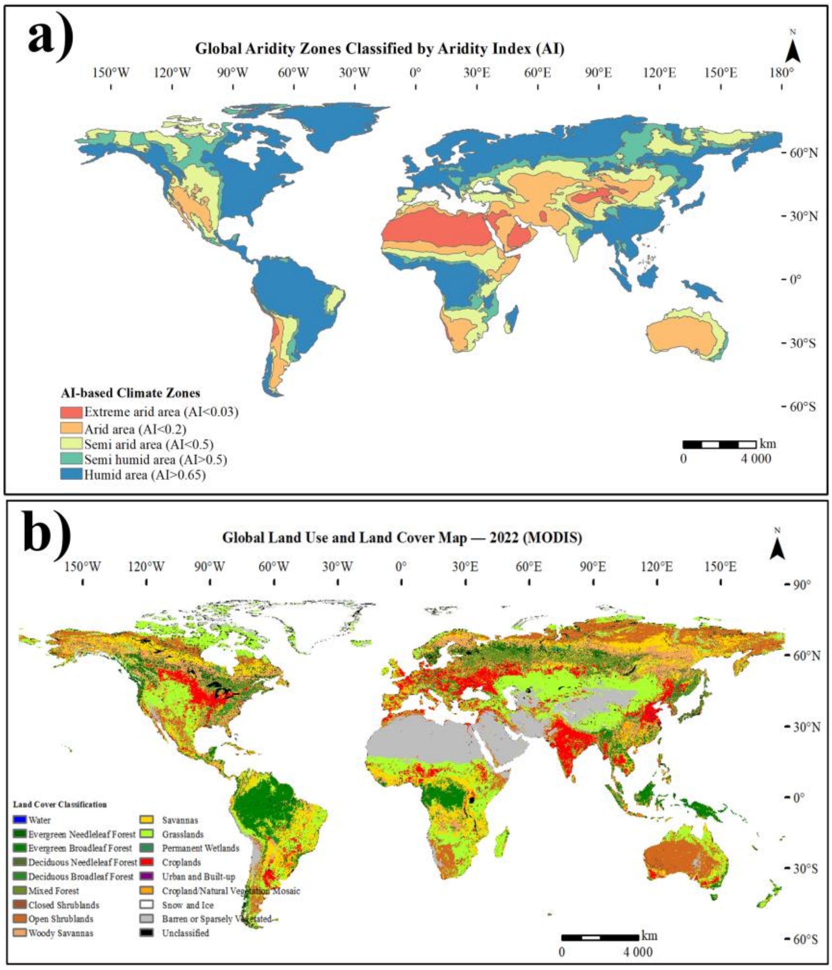

Figure 1. (**a**) Classification of global drylands based on the Aridity Index (AI); (**b**) Global land use in 2022.

The hydrological cycle refers to the continuous movement and transformation of water among the Earth's spheres [3] (Figure 2). In drylands, precipitation constitutes the primary source of water [4], while evapotranspiration is the dominant pathway of water loss [5,6]. Soil moisture regulates root-zone water availability for vegetation, and groundwater serves as a crucial supplementary resource during dry seasons [7]. Variations in the hydrological cycle of drylands arise from the combined effects of climate change, human activities, and natural variability. Global warming is reshaping both the intensity and pattern of the water cycle: higher temperatures enhance evapotranspiration, increase atmospheric water-holding capacity, and accelerate overall water circulation. In drylands, intensified soil and vegetation evapotranspiration, coupled with limited and uneven precipitation gains, leads to soil moisture deficits and aggravated droughts [8]. Human groundwater pumping and large-scale ecological restoration further contribute to groundwater depletion [9–11]. At the same time, atmospheric circulation and monsoon systems transport the limited water vapor from drylands to other regions, thereby disrupting local water balance and worsening moisture scarcity [12]. In summary, climate change functions as the overarching driver of hydrological change in drylands, while human activities and vegetation dynamics act as regional modulators. Their interactions jointly determine the evolutionary trajectory of hydrological processes in these regions.

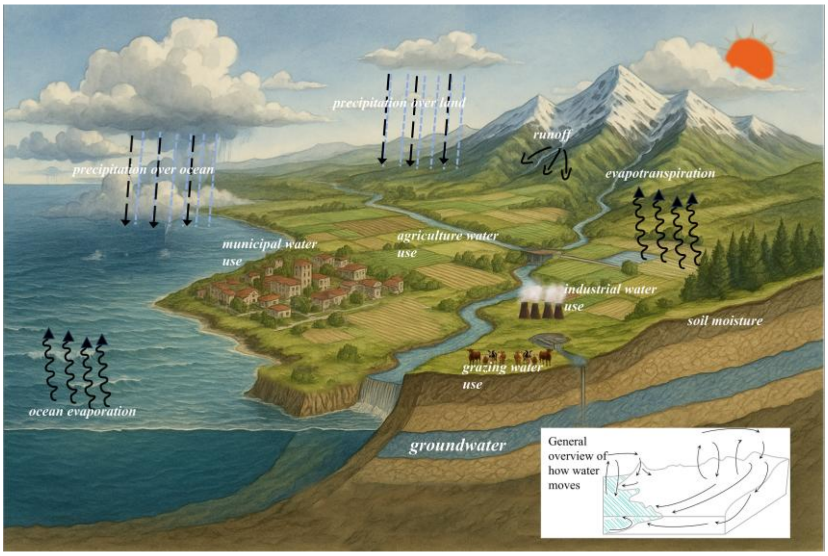

Figure 2. Schematic representation of the hydrological cycle.

However, traditional hydrological monitoring methods, such as hydrological and meteorological stations, are constrained by short observational records and limited spatial coverage, making it difficult to capture large-scale dynamics of hydrological processes in drylands [13,14]. In recent years, advances in remote sensing technologies have enabled increasing use of satellite observations to quantify hydrological changes in drylands [15,16]. As Chen, et al. noted, remote sensing can provide high-frequency and long-term meteorological and environmental datasets, offering rich spatial information for hydrological model inputs [17]. Cheng, et al. further emphasized that reanalysis products, by integrating ground-based observations with numerical weather models, deliver hydrometeorological information with strong continuity and broad spatial coverage [18].

The objective of this review is to synthesize multi-source remote sensing data to assess the spatiotemporal dynamics of the hydrological cycle in drylands and to examine the driving mechanisms. Specifically, it aims to:

(1) review the role of multi-source remote sensing data in quantifying the spatiotemporal variability of the hydrological cycle in drylands;
(2) summarize the observed spatiotemporal characteristics and driving mechanisms of hydrological change in drylands.

2. Bibliometric Analysis

To examine the evolutionary characteristics of the hydrological cycle in drylands, we conducted a bibliometric search using hydrological keywords such as evapotranspiration, precipitation, soil moisture, and groundwater, combined with remote sensing–related terms including remote sensing and GRACE. We further restricted the scope to research themes such as arid regions, drylands, and water scarcity. The search was carried out in May 2025 across three major databases—Web of Science, ScienceDirect, and SpringerLink—yielding 943, 4546, and 6903 publications, respectively. All retrieved records were imported into EndNote 20, where duplicate entries were initially removed using the “Find Duplicates” function. Clear inclusion and exclusion criteria were then applied. Eligible studies met the following conditions: (1) the study area was located in hyper-arid, arid, or semi-arid regions; (2) multi-source remote sensing data (e.g., TRMM/GPM, MODIS, SMAP, GRACE) were employed; (3) at least two hydrological variables (e.g., precipitation, evapotranspiration, soil moisture, groundwater, or TWS) were analyzed; and (4) the publication year was 2000 or later. Conversely, we excluded studies that focused solely on a single hydrological variable without integrative analysis, addressed only vegetation or ecological dynamics without linking them to the hydrological cycle, or relied exclusively on ground observations or model simulations without incorporating remote sensing or reanalysis data. In total, 292 studies met these criteria (Figure 3). Their keywords were further analyzed using VOSviewer to generate maps of keyword co-occurrence and temporal evolution (Figure 4). Figure 4 shows that research on hydrology in drylands has increased year by year, with climate change, remote sensing, and drought emerging as major themes and recent hotspots. These patterns indicate that hydrological studies in drylands are attracting growing scholarly attention. We categorized the study areas of these papers by continent (Figure 5). However, papers with a global research scope are specifically represented in the pie chart of the figure. We found that studies with a global coverage account for the largest proportion, followed by Asia and North America, Africa also emerges as an important research hotspot.

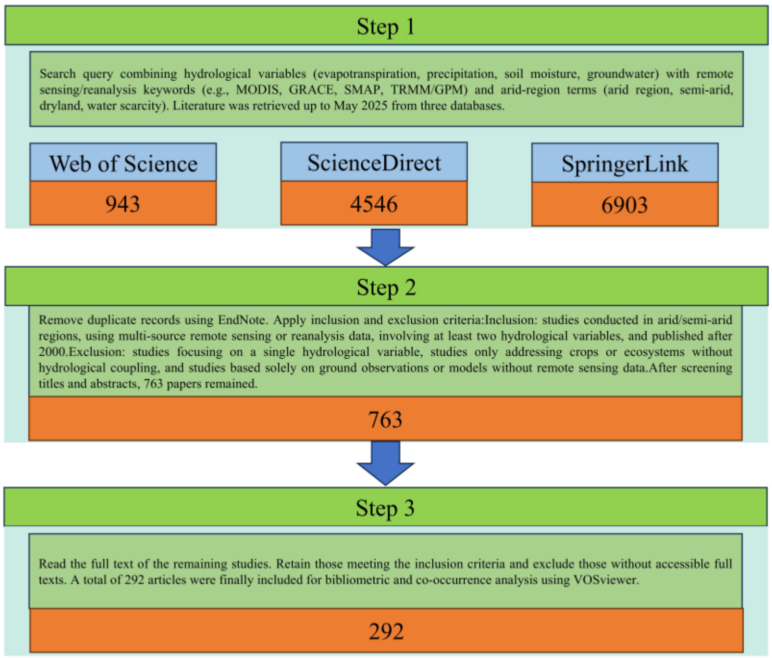

Figure 3. The operational steps for systematically organizing and summarizing publications.

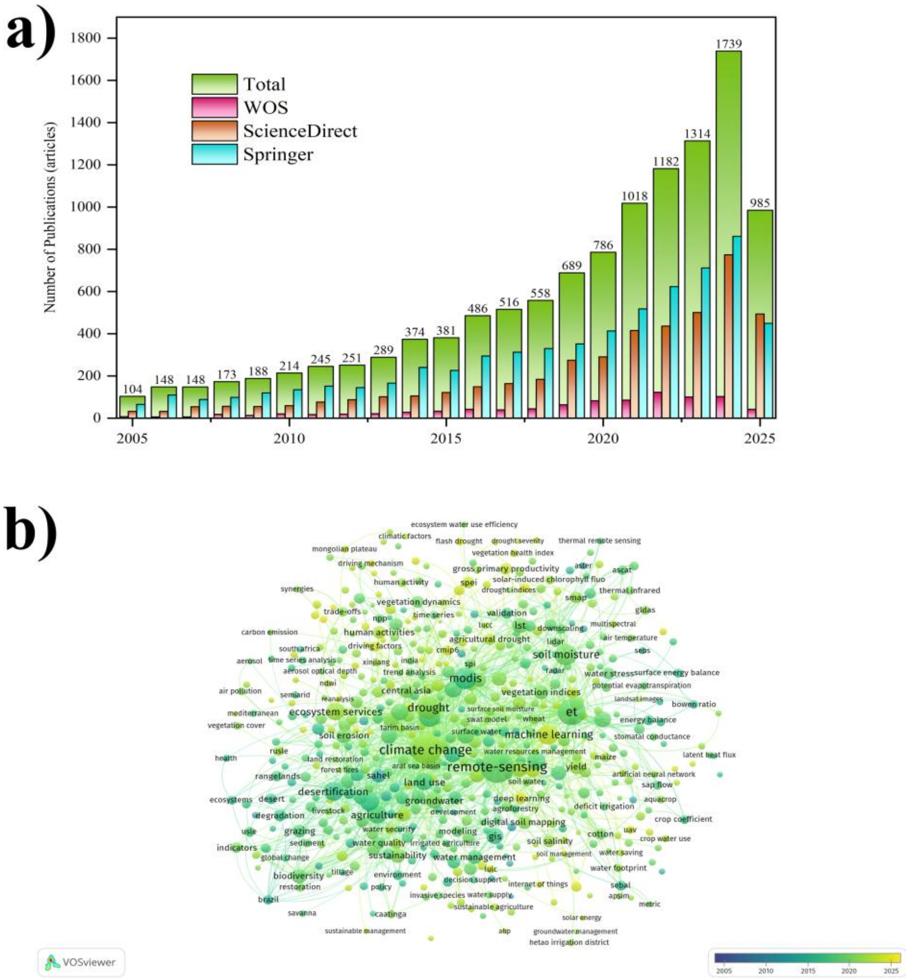

Figure 4. (**a**) Bar chart of the number of database papers; (**b**) Keyword co-occurrence relationship diagram.

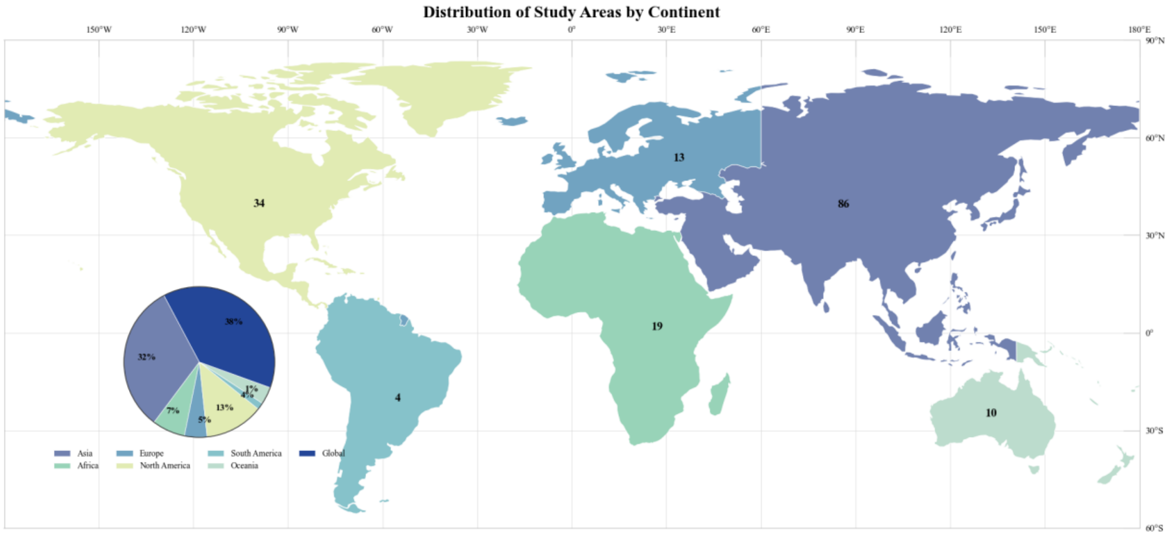

Figure 5. Distribution of study areas by continent (excluding global-scale studies).

3. Comparison of Remote Sensing Data Products

For monitoring hydrological processes in drylands, a wide range of representative remote sensing and reanalysis products have been developed. A timeline of the major datasets is presented in Figure 6. Table 1 provides a comparative overview of typical products for precipitation, evapotranspiration, soil moisture, groundwater, and vegetation indices, summarizing their characteristics, strengths, limitations, and representative applications in drylands. Overall, satellite remote sensing products offer high spatiotemporal resolution and broad coverage, making them suitable for monitoring surface dynamics in drylands. Reanalysis products, in contrast, provide long-term continuity and multi-variable consistency, which are advantageous for analyzing the climatic drivers of hydrological processes in drylands. Nevertheless, differences exist among datasets in terms of their adaptability to the distinctive climatic conditions, scales, and research needs of drylands, and careful selection or integration is required according to specific study objectives.

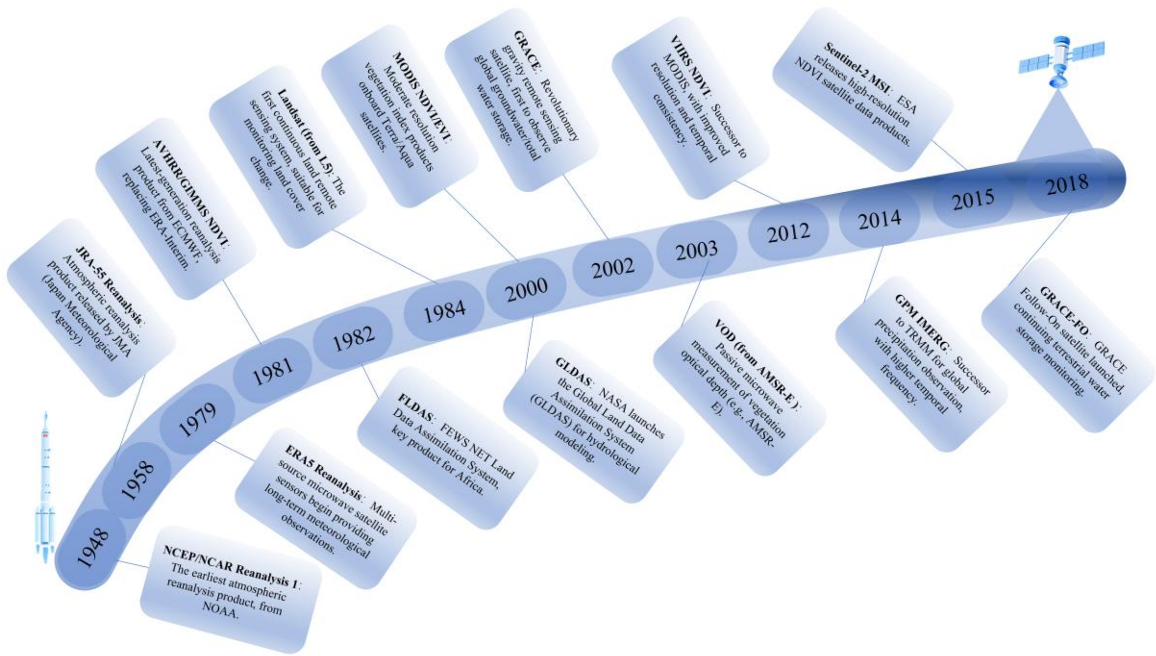

Figure 6. Timeline of major remote sensing data products.

Table 1. Comparison of remote sensing data products.

Hydrological Variable	Dataset/Product	Spatiotemporal Resolution	Advantages	Limitations	Typical Applications in Drylands
Precipitation (P)	TRMM 3B42	0.25°, 3 h	High temporal frequency; multi-sensor fusion; suitable for monitoring convective rainfall	Bias in extreme rainfall; limited spatial resolution	Daily precipitation monitoring; drought index calculation; early warning of heavy rainfall
	CHIRPS	0.05°, daily–monthly	Long-term record (1981–present); high spatial accuracy; integrates gauge observations	Larger errors in hyper-arid regions; latency in updates	Drought monitoring; rainy season trend analysis; widely applied in African and Asian drylands
	ERA5, MERRA-2 (reanalysis)	~0.25–0.5°, hourly	Complete spatiotemporal coverage; physically consistent	Overestimation of convective rainfall; smoothed local variability	Climate trend analysis; large-scale water cycle modeling
Evapotranspiration (ET)	MODIS MOD16A2	500 m, 8-day	Moderate–high spatial resolution; global coverage	Cloud contamination; less robust in arid areas	Drought monitoring; regional ET estimation
	GLEAM	0.25°, daily	Multi-source fusion; considers vegetation and soil moisture stress; distinguishes potential vs actual ET	Coarse resolution; limited sensitivity to local processes	Global drought assessment; long-term ET trend analysis
	GLDAS Noah	0.25°, 3 h–monthly	Provides multi-variable ET estimates; strong internal consistency	No representation of human water use; depends on forcing data	Drought monitoring; water balance studies
Soil moisture (SM)	SMAP	9–36 km, daily	High accuracy; near-real-time retrieval of surface (~0–5 cm) soil moisture	Short time series; shallow penetration	Surface soil moisture monitoring; crop water stress assessment
	ESA CCI SM	0.25°, daily	Long-term record (1978–present); multi-sensor harmonization	Coarse resolution; lacks deep soil layers	Drought trend assessment; climate change studies
	GLDAS, ERA5-Land	0.1–0.25°, hourly	Multi-layer soil moisture estimates	Bias from forcing data and model assumptions	Regional water balance; model intercomparison
Groundwater/Terrestrial water storage (GWS/TWS)	GRACE/GRACE-FO	~300 km, monthly	Direct observations of TWS anomalies; long-term consistency	Coarse resolution; requires signal decomposition	Aquifer depletion monitoring; water storage deficit trends
	JPL Mascon	0.5°, monthly	Improved signal-to-noise ratio; suitable for basin-scale analysis	Still limited for small catchments	Groundwater change assessment; regional water balance
Vegetation (NDVI and water stress indicators)	MODIS NDVI/EVI	250–500 m, 16-day	Long-term global coverage; relatively high accuracy	Cloud contamination; NDVI saturation in dense vegetation	Monitoring vegetation response to precipitation; greening–browning trends
	AVHRR GIMMS NDVI	8 km, biweekly, 1981–2015	Longest NDVI record available	Coarse resolution; sensor degradation and drift	Historical vegetation change analysis in drylands
	Sentinel-2 NDVI	10–20 m, 5-day	High spatial resolution; captures local vegetation patterns	Short record; requires preprocessing	Irrigated area and oasis monitoring; fine-scale crop studies
	VOD (AMSR-E/SMAP)	~0.25°, daily–monthly	Sensitive to vegetation water content; strong penetration ability	Coarse resolution; coupled with soil moisture	Vegetation water stress monitoring; complementary to NDVI

4. Characteristics and Driving Mechanisms of Hydrological Changes in Drylands

4.1. Precipitation

Using ERA5 data, we mapped the global distribution of mean annual precipitation for 2001–2022 (Figure 7a). The results show that equatorial regions, particularly the Amazon Basin, Central Africa, and Southeast Asia, receive precipitation well above the global average, exceeding 2000 mm yr^{-1}. In contrast, arid and semi-arid regions such as North Africa, Central Asia, the Australian interior, and the Arabian Peninsula are characterized by scarce rainfall, generally below 400 mm yr^{-1}, reflecting distinct spatial differentiation. The gradient from red to blue in the figure clearly illustrates the zonal pattern of global moisture transport, with a pronounced precipitation gradient between mid-latitude drylands and tropical humid regions. At the same time, the interannual trend of global mean precipitation indicates a gradual increase since 2001, with a regression slope of 0.62 mm yr^{-1}. This trend passes both the Mann–Kendall (MK) test ($p = 0.048$) and the linear regression t-test ($p = 0.033$). Given that global hydrometeorological datasets (e.g., ERA5) often exhibit non-normal distributions, serial dependence, and heteroscedastic variance, the non-parametric MK test was adopted as the primary approach for trend detection because it does not assume normality and is less sensitive to outliers. The consistent significance obtained from both methods confirms the robustness of the upward trend. For methodological consistency, the MK test was also applied to all subsequent variables (evapotranspiration, soil moisture, groundwater, and terrestrial water storage). Despite substantial interannual variability and the superposition of multi-scale climate signals, the overall increase in global precipitation remains statistically reliable, likely linked to the intensification of the atmospheric water cycle under global warming, though its specific implications for drylands require further investigation.

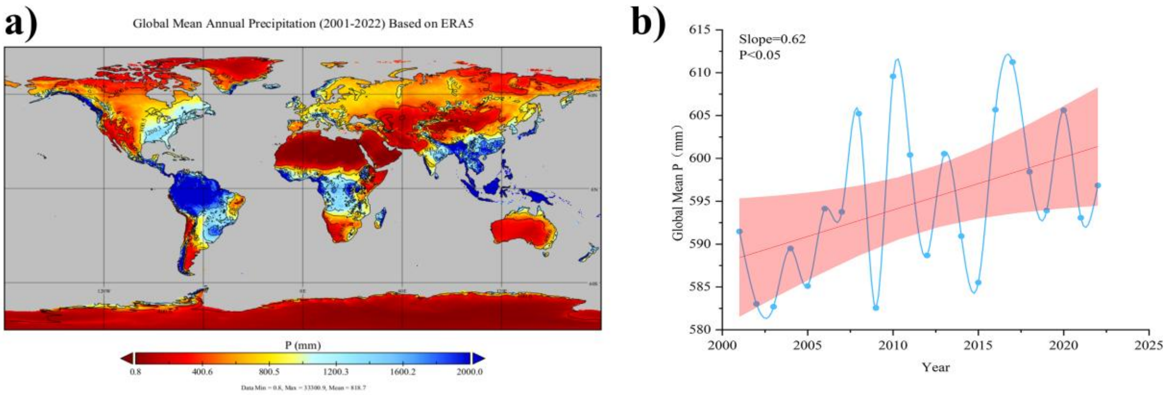

Figure 7. (**a**) spatial distribution of mean annual precipitation; (**b**) interannual trend of global mean annual precipitation.

In some regions, precipitation has increased. Northwestern China and Central Asia, for example, have experienced a “warm–wet” trend since the late twentieth century, with annual precipitation showing a rising tendency. Statistics indicate that since the mid-twentieth century, precipitation in these areas has increased significantly, at a rate of approximately 1–2 mm per decade [19]. In the African Sahel, rainfall began to recover in the 1990s following the severe droughts of the 1970s and 1980s. As noted by Park, et al., this “partial recovery” is thought to be linked to nearby ocean warming [20]. By contrast, other dryland regions have seen continued or prolonged precipitation declines. In the North African subtropical drylands, precipitation has generally decreased in recent decades, maintaining a “warm–dry” climatic regime. The southwestern United States experienced a relatively wet phase during the latter half of the twentieth century, but since the early twenty-first century rainfall has diminished, and the ongoing “megadrought” underscores the region’s persistent water deficit [19]. Precipitation trends in the Australian interior and surrounding drylands vary by location: most of the inland areas show little long-term change in mean precipitation, yet interannual variability is extremely high and extreme droughts occur frequently. In southwestern Australia, winter–spring rainfall has declined markedly since the 1970s, a drying trend attributed to changes in Southern Hemisphere circulation. Southeastern Australia also suffered the severe “Millennium Drought” between 1997 and 2009, when annual precipitation decreased by about 9% [21], placing immense pressure on regional water resources.

Precipitation in drylands exhibits pronounced seasonality and strong interannual variability [19,22]. In mid-latitude continental drylands, rainfall is concentrated in the cold seasons of winter and spring, with winter atmospheric circulation exerting a major influence. Yan et al. noted that regardless of proximity to the coast, precipitation in mid-latitude drylands is largely confined to the winter half-year [19]. In contrast, low-latitude drylands receive most of their rainfall during the summer wet season, associated with the seasonal northward migration of the Intertropical Convergence Zone, resulting in distinct wet and dry periods within a year [23,24]. On the interannual scale, precipitation variability is strongly modulated by internal oscillations of the climate system. In the Sahel, the prolonged drought of the late twentieth century and subsequent partial recovery illustrate the role of decadal-scale ocean temperature anomalies in regulating regional rainfall [25]. In the southwestern United States and North Africa, decadal fluctuations are often out of phase: when rainfall decreases in North Africa, it tends to increase in the U.S. Southwest, and vice versa [19]. This negative correlation is attributed to the influence of large-scale ocean–atmosphere oscillations on regional circulation patterns. Overall, precipitation in drylands is characterized by highly uneven spatial and temporal distribution. The pattern of "increasing in the east and decreasing in the west, with pronounced temporal fluctuations" represents a typical feature of precipitation change in many dryland regions.

4.2. Evapotranspiration

Against the background of global warming, evapotranspiration (ET) in drylands has generally increased. Rising temperatures enhance the atmosphere's capacity to hold and evaporate water, elevating the vapor pressure deficit (VPD) and thereby increasing evaporative demand [8]. Numerous studies have pointed out that in drylands, warming tends to raise potential evapotranspiration more rapidly than precipitation, and this imbalance—where the increase in evaporation exceeds the increase in rainfall—is a major driver of intensifying drought. Yan et al. reported that in the southwestern United States, annual precipitation has slightly decreased since the early twenty-first century, while ET has risen substantially, shifting the regional climate from relatively moist to markedly drier conditions [19]. Global reanalysis datasets similarly indicate that since the 1960s many already arid regions have experienced significant ET increases, thereby intensifying climatic aridity [8]. Figure 8b illustrates the annual trend of global mean ET during 2001–2022, derived from MODIS MOD16A2 monthly products with a spatial resolution of 0.1°. The trend line shows a significant increase over the past two decades, with Sen's slope estimating a rise of approximately 2.26 mm per year. This indicates that ET activity has intensified globally, likely driven by the combined effects of rising temperature, vegetation change, and enhanced water cycling. Figure 8a further presents the spatial distribution of mean annual ET over the same period. High ET values occur mainly in tropical rainforests such as the Amazon Basin, the Congo Basin, and Southeast Asia, where annual ET exceeds 1000 mm. In contrast, arid and cold regions—including the Sahara, the Arabian Peninsula, northwestern China, and Greenland—exhibit low or even missing values. The absence of ET estimates in some areas reflects the MODIS MOD16A2 quality control procedure, which masks pixels in permanent snow/ice regions and under persistent low-quality retrieval conditions. These masked pixels remain as no-data values. Together, these two figures clearly reveal the spatiotemporal evolution of ET at the global scale, providing critical evidence for understanding the interactions between surface water balance and climate change.

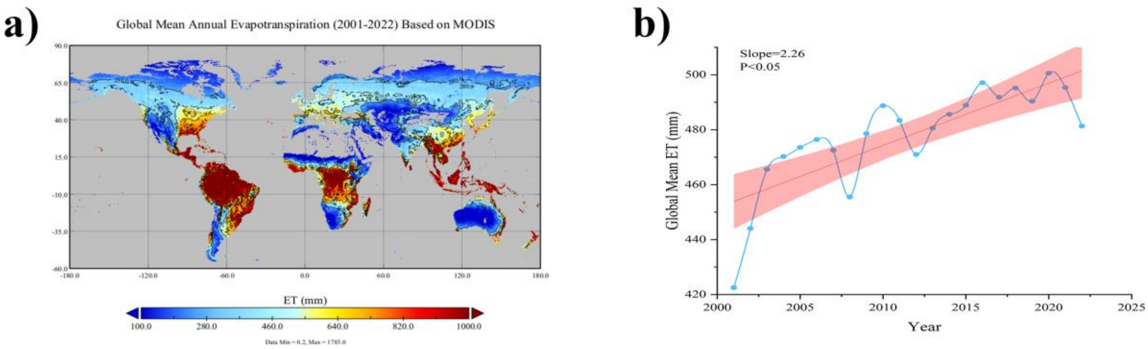

Figure 8. (**a**) Spatial distribution of global mean annual evapotranspiration; (**b**) interannual trend of global mean evapotranspiration.

ET is controlled not only by atmospheric demand but also by water availability. In periods or regions with sufficient moisture, warming promotes increases in actual ET; under extreme aridity, however, water deficits in soils and vegetation constrain ET from reaching its potential. In recent years, ET trends across drylands have diverged. In regions where precipitation has increased, improved soil moisture and vegetation cover have enhanced ET, whereas in areas with persistently low rainfall, water scarcity has restricted ET growth or even caused declines [8]. For example, in northwestern China and parts of Central Asia, greater precipitation and vegetation "regreening" [26] have strengthened land–atmosphere water exchanges [27,28]. In contrast, long-term drought in the southwestern

United States and parts of Australia has dried soils, limiting ET increases [29]. Vegetation dynamics further reflect these differences. Satellite observations show rising vegetation cover in the Sahel and Central Asian Plateau, suggesting improved local water conditions, while declines in cover have been observed in southwestern North America, South American dry grasslands, Mongolia, and parts of inland Australia due to worsening drought. These patterns indicate that not all drylands are becoming uniformly drier; hydrological responses are regionally differentiated. Overall, in water-limited drylands, warming-driven increases in atmospheric evaporative demand rarely translate into proportional ET increases, and instead exacerbate water deficits. With further warming and intensifying drought, many regions now exhibit the co-occurrence of higher vapor pressure deficit (VPD) and lower soil moisture, signaling that vegetation and soils are under growing drought stress [30]. Consequently, changes in ET substantially amplify hydrological imbalances in drylands and constitute a key process for understanding shifts in their water cycle.

4.3. Soil Moisture

Soil moisture in drylands is a key indicator of terrestrial dryness and vegetation drought stress. Recent studies based on soil moisture observations and model reconstructions have reported an overall global decline [7]. Satellite microwave remote sensing analyses indicate that global surface soil moisture decreased during 1979–2013. Approximately 30% of the global land surface exhibited significant soil moisture trends, with about 22% becoming drier and only 7% wetter [31]. Notably, these soil moisture changes do not fully conform to the “dry gets drier, wet gets wetter” paradigm; instead, the more prominent feature is “drylands get drier,” with over half of the drying trends occurring in already arid regions. Seo, et al. further estimated that between 2000 and 2002 global soil moisture declined by roughly 1614 Gt—nearly twice the mass loss of the Greenland Ice Sheet during the same period—and argued that under current climate conditions, soil moisture recovery is unlikely [32]. This study employed the NASA/GLDAS/V021/NOAH/G025/T3H dataset to obtain global soil moisture at 0–40 cm depth by combining the 0–10 cm and 10–40 cm layers. Annual averages from 2001 to 2022 were calculated. Before deriving the global mean, soil moisture values were limited to the range of 0–2000 mm to remove abnormal or missing records, and the data were resampled to a uniform spatial resolution of 25 km to ensure consistency. As shown in Figure 9, soil moisture displays clear spatial heterogeneity across different climate zones. High soil moisture levels (>160 mm) are mainly distributed in tropical humid regions, including the Amazon Basin, the Congo Basin, and Southeast Asia, where strong rainfall and active hydrological cycles dominate. In contrast, extremely low values (<50 mm) are observed in arid regions such as the Sahara Desert, Central Asia, the southwestern Asian Plateau, and central Australia, reflecting severe surface dryness. Mid-latitude areas—such as central North America, eastern and central Europe, the Chinese Loess Plateau, and the North China Plain—maintain moderate soil moisture (85–150 mm), strongly affected by seasonal precipitation and vegetation cover. In high-latitude regions, particularly around the Arctic permafrost zone, soil moisture is largely controlled by temperature, and local maxima are related to freeze–thaw processes. These spatial features reveal the pronounced heterogeneity of global soil moisture and its importance for hydrological-climatic monitoring and drought evaluation.

At the regional scale, soil moisture in the Eurasian dry belt has generally declined, accompanied by a marked increase in evaporative demand. Zhang et al. reported that in recent years the Eurasian drylands have experienced simultaneous decreases in soil moisture and increases in vapor pressure deficit (VPD), indicating intensifying soil drought [30]. This pattern is consistent with the combined effects of rising temperatures and insufficient precipitation. In northwestern China and Central Asia, although increased rainfall has partly enhanced soil wetness, the rapid rise in temperature and evapotranspiration has offset much of this effect. As a result, changes in the aridity index remain relatively stable, reflecting a “warming and slightly wetter but not significantly waterlogged” condition. In contrast, in regions such as North Africa and the Middle East where precipitation has continued to decline, soil moisture conditions have worsened, with drier soils during the dry season making vegetation maintenance increasingly difficult. This, in turn, elevates land surface temperatures and sensible heat fluxes, reinforcing a vicious cycle. In the southern Great Plains and southwestern United States, deep soil moisture has also decreased, with faster depletion and slower recovery during droughts, adversely affecting agricultural production and grassland ecosystems.

Seasonal fluctuations in soil moisture are directly linked to crop cultivation and pasture growth. In many dryland regions, the onset, duration, and peak of soil moisture during the rainy season have shifted in recent decades. In the Sahel, rainfall recovery has raised peak soil moisture levels during the wet season compared with the severe droughts of the late twentieth century, slightly extending the growing season. In the Australian interior, La Niña events have produced intense rainfall episodes that temporarily boosted surface soil moisture and triggered vigorous vegetation growth, but subsequent El Niño phases quickly drove soils back into dryness. Overall, soil moisture acts as a "buffer" to precipitation, with changes lagging behind rainfall inputs, yet its long-term trajectory reflects evolving regional hydroclimatic conditions. Continued warming is reducing soil moisture-holding capacity, making dryland soils more prone to desiccation and thereby heightening the risks of agricultural drought and desertification.

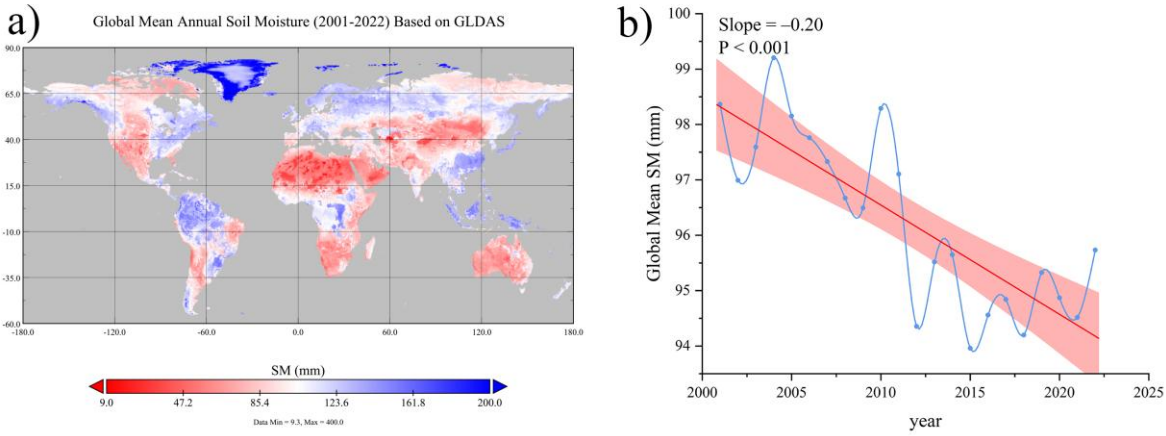

Figure 9. (**a**) Spatial distribution of global mean annual soil moisture; (**b**) interannual trend of global mean soil moisture.

4.4. Groundwater and Terrestrial Water Storage

Groundwater and terrestrial water storage (TWS) serve as the most important long-term water reservoirs maintaining hydrological balance in drylands. In these regions, surface water is limited and ephemeral; thus, TWS variations mainly reflect changes in groundwater storage. Using the High-Resolution Water Storage Anomaly (HWSA v1.0) dataset and GRACE/GRACE-FO satellite observations [33], we analyzed global patterns of groundwater storage anomalies (GWSA) and terrestrial water storage anomalies (TWSA) from 2002 to 2022 (Figures 10 and 11). The results reveal widespread depletion of groundwater and total water storage across global drylands. Severe groundwater losses are found in northern India, Pakistan, Iran, Central Asia, the North China Plain, and the western United States, with annual depletion exceeding 60 mm, reflecting long-term overexploitation for irrigation under limited recharge. Cumulative losses in several basins exceed 300 mm (Figure 10b), underscoring the persistence of groundwater decline during the past two decades. Globally, GWSA exhibits a significant decreasing trend of −2.18 mm yr^{-1} (Figure 10c), closely associated with groundwater overpumping, land-use change, and recurrent drought. The spatial patterns of TWSA (Figure 11) are highly consistent with those of GWSA, confirming that in drylands, total water storage decline primarily mirrors groundwater depletion. The Middle East, Central Asia, northern India, and inland Australia show the largest decreases (>60 mm yr^{-1}), reflecting the combined effects of groundwater drawdown and reduced soil-water content.

These findings are consistent with ground-based observations. Jasechko, et al. reported that 36% of global aquifers declined faster than 0.1 m yr^{-1} over the past four decades, with 12% falling faster than 0.5 m yr^{-1}—mainly in arid and semi-arid agricultural regions [34]. GRACE observations further indicate that groundwater storage in northern India and Pakistan has declined at rates of 0.3–0.6 m yr^{-1} since 2002, ranking among the most depleted regions globally. Similar depletion occurs in the North China Plain and northwestern oases, where shallow aquifers have dropped by tens of meters and deep aquifers by more than 1 m yr^{-1} in some irrigated zones. These areas, where surface water is scarce and dependence on groundwater is excessive, have already experienced cone-of-depression formation and land subsidence [35]. In Middle Eastern and North African countries, large-scale abstraction of fossil groundwater for agriculture and domestic use, coupled with minimal rainfall recharge, has led to continuous groundwater decline and the shrinkage of desert oases [36]. In California's Central Valley and the lower Colorado River Basin, recurrent droughts have intensified groundwater pumping to offset surface water shortages, causing rapid depletion of groundwater reserves [37].

Groundwater responds slowly to climatic and anthropogenic forcing. Compared with precipitation and soil moisture, its recovery is extremely limited once depleted. In many drylands, human extraction far exceeds natural recharge, while climate warming further reduces infiltration and enhances evaporation, weakening replenishment capacity. For example, Australian drylands experience little to no groundwater recharge during drought years [38,39], and recharge in the U.S. Southwest has declined due to reduced snowmelt from mountain regions [37]. These persistent declines in both groundwater and total water storage highlight the dual impact of climate-driven aridification and human overexploitation, posing serious challenges for water security and sustainable management in global drylands.

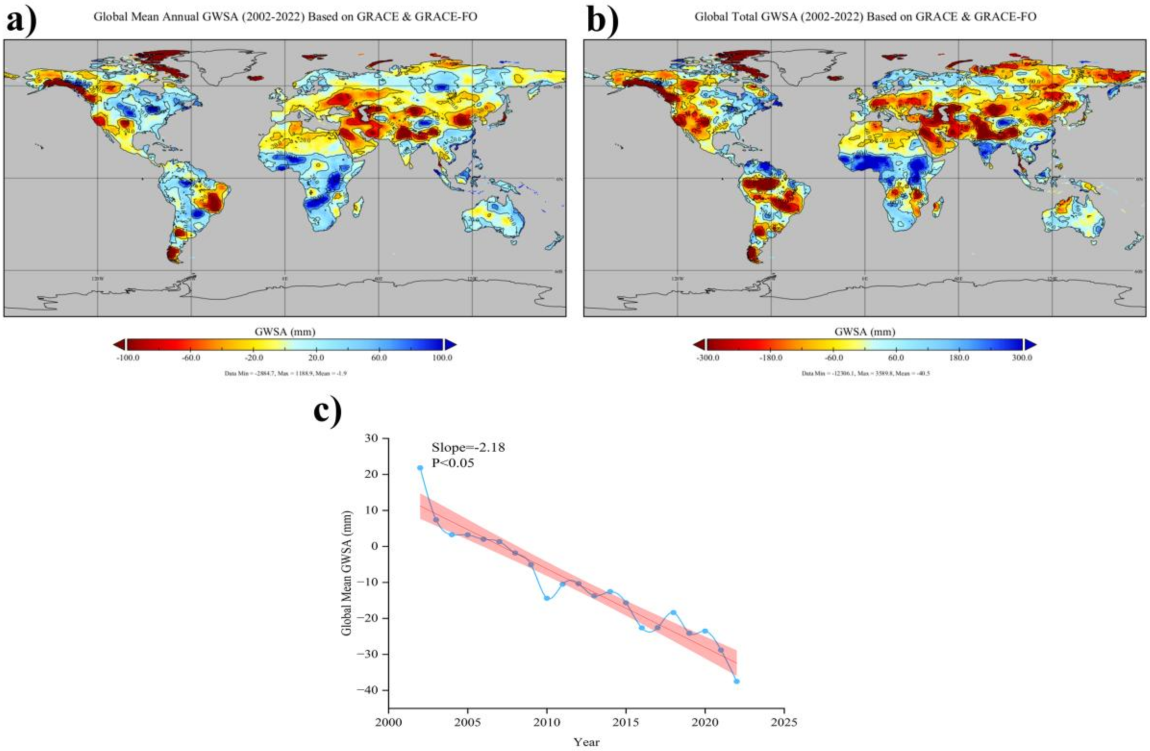

Figure 10. (**a**) Spatial distribution of global mean annual groundwater storage anomalies; (**b**) cumulative spatial pattern of total groundwater storage anomalies; (**c**) interannual trend of global average GWSA.

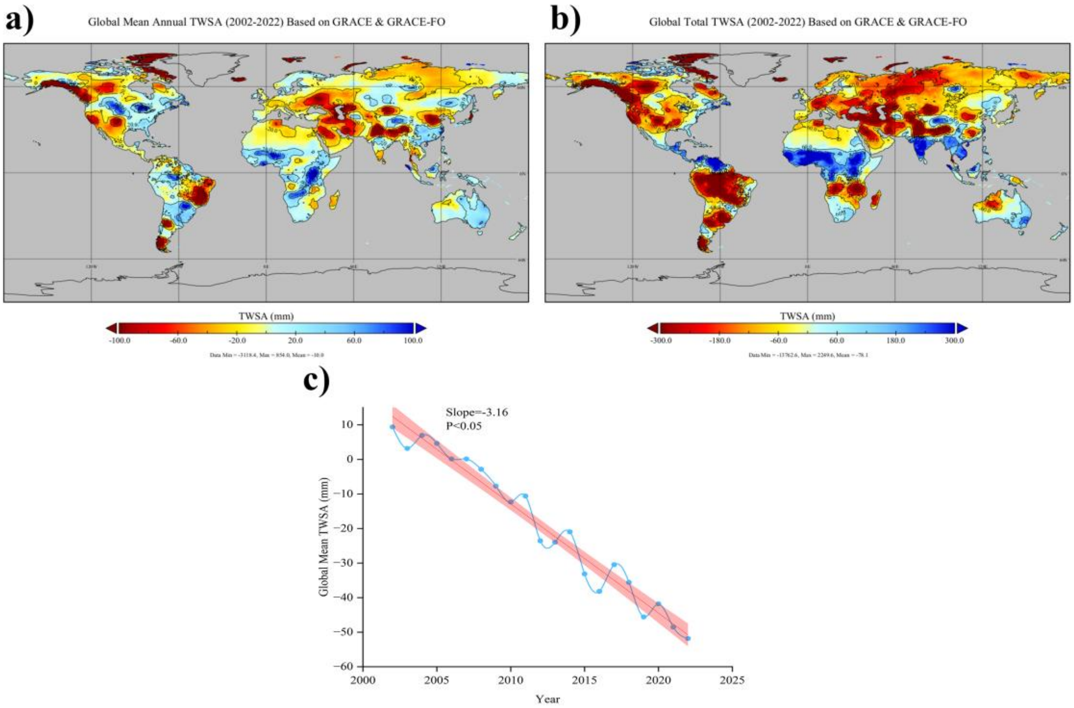

Figure 11. (**a**) Spatial distribution of global mean annual TWSA; (**b**) cumulative spatial distribution of total TWSA; (**c**) interannual trend of global average TWSA.

4.5. Runoff

This study derived annual total runoff depth by summing ERA5-Land monthly runoff for 2001–2022 and, at 10-km resolution, computes the multi-year mean spatial pattern and the land-area-weighted global annual series (Figure 12). The multi-year mean shows a pattern of high values in humid low latitudes and high-latitude snowmelt regions, and low values in arid belts: the Amazon and Congo basins, the Southeast Asian monsoon region, and high-latitude zones in North America and Eurasia are high; the Sahara, Central–West Asia, Australia's interior, and western South Africa are near zero. This pattern aligns with the distributions of precipitation and evapotranspiration; in arid regions, scarce precipitation and strong evaporative demand limit runoff generation. Interannually, the land-area-weighted global annual total runoff exhibits a modest upward trend over 2001–2022, with a slope of about 0.01 mm yr^{-1} (Figure 12b). Based on the spatial context, most of the increase occurs outside arid belts—in humid low latitudes and high latitudes—whereas arid regions contribute little, given their low multi-year means and weak or negligible pixel-scale trends.

Combining this with the preceding analyses of hydrological variables, three points follow: first, humid low latitudes see more frequent and intense extreme rainfall, which elevates annual runoff; second, in mid- to high-latitudes, warming coupled with precipitation changes enhances snowmelt and rainy-season runoff; finally, in arid belts, low precipitation combined with high evapotranspiration dominates, so additional water is more often consumed by evaporation and transpiration than converted to runoff.

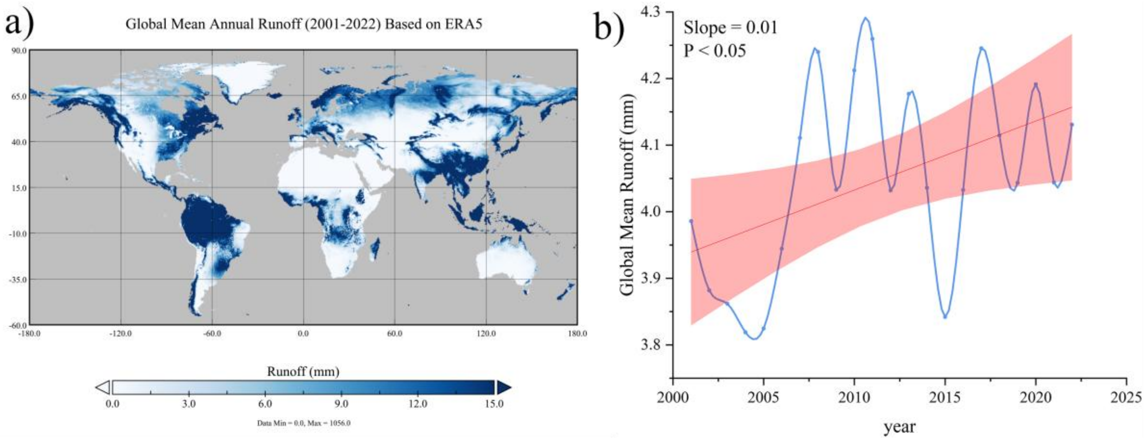

Figure 12. (**a**) Spatial distribution of global mean runoff; (**b**) interannual trend of global mean runoff.

4.6. Driving Mechanisms

Changes in hydrological variables in drylands result from the combined effects of climatic factors and human activities. The main drivers include global warming, shifts in atmospheric circulation, decadal climate oscillations, and anthropogenic influences such as land use and water utilization (Figure 13).

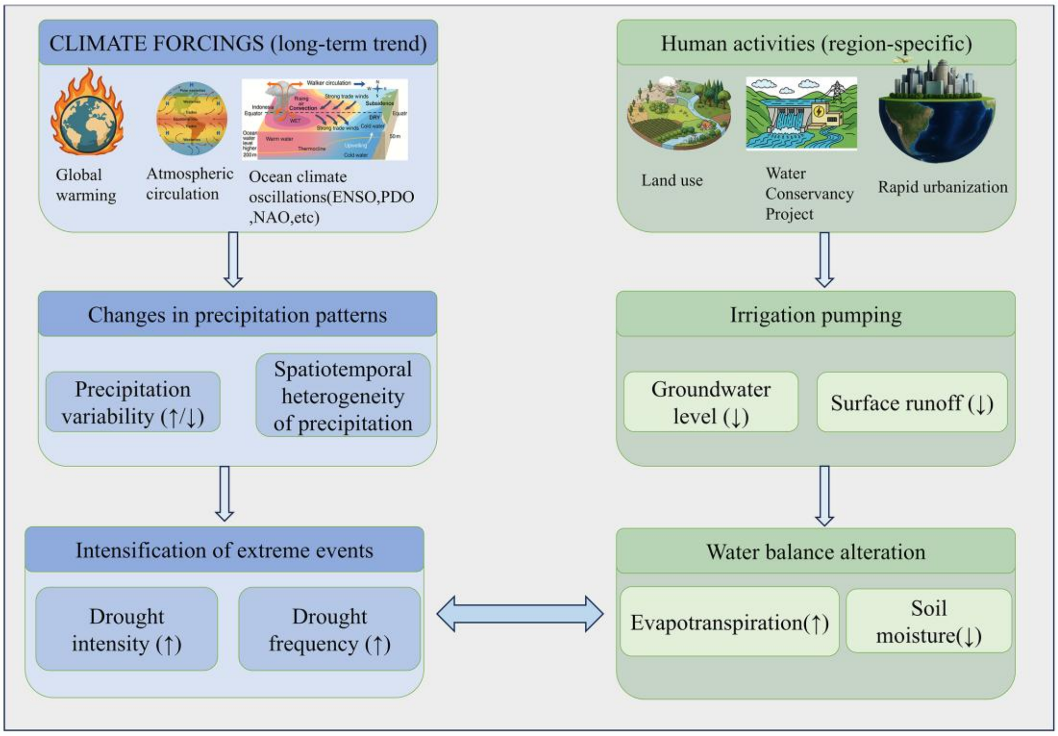

Figure 13. Conceptual framework illustrating the driving mechanisms of hydrological variables in drylands.

Global warming exerts the most direct influence on the hydrological cycle of drylands. Rising temperatures enhance atmospheric evaporative capacity, and increases in potential evapotranspiration intensify terrestrial water loss [8]. When precipitation remains stable or increases only modestly, this leads to greater regional aridity, making drylands even drier. Warming also alters large-scale circulation patterns [40]. Tamarin-Brodsky and Kaspi demonstrated, based on both observations and models, that the subtropical high-pressure belt has strengthened and shifted poleward in recent decades, a characteristic response to climate warming [41]. As a result, mid-latitude moist airflows are displaced toward higher latitudes, while subtropical arid zones expand poleward. This phenomenon is evident in both hemispheres. In the Southern Hemisphere, since the mid-twentieth century, storm tracks during austral winter and spring have shifted southward [42], with strengthened high-pressure systems reducing rainfall in southern Australia. In the Northern Hemisphere, rainfall belts over North Africa and the Mediterranean have retreated southward, while westerly circulation over Central Asia has weakened [43], leading to reduced or more variable precipitation in these regions. Such circulation adjustments partly explain the persistent drying observed since the 1970s in southwestern Australia and along the Mediterranean coast. In addition, global warming increases atmospheric moisture content, which may enhance precipitation in some monsoon-margin regions, indicating that warming can have both positive and negative effects on rainfall. Overall, however, in drylands warming tends to amplify extremes, with higher temperatures producing more severe droughts and more intense rainfall events. These patterns are consistent with the observed uneven distribution and growing extremity of precipitation across drylands.

Large-scale ocean–atmosphere oscillations play a critical role in modulating interannual to decadal hydrological variability in drylands [44,45]. Among them, the El Niño–Southern Oscillation (ENSO) is the most influential factor. During El Niño events, precipitation belts in the western Pacific and Indian Ocean shift eastward, often resulting in substantial rainfall reductions over Australia, Southeast Asia, southern Africa, and the Amazon, triggering droughts. Conversely, La Niña phases tend to increase rainfall in these regions while causing abnormal dryness in the southwestern United States and northern Mexico. Such ENSO-driven precipitation anomalies have recurred throughout historical records and represent a primary source of interannual drought–flood oscillations in drylands. The heightened frequency of ENSO events in recent decades has corresponded with severe hydroclimatic extremes in multiple regions. Beyond ENSO, low-frequency modes such as the Pacific Decadal Oscillation (PDO) and the Atlantic Multidecadal Oscillation (AMO) also exert significant impacts on precipitation trends in drylands. Yan et al. demonstrated that PDO phases are closely linked to precipitation variability in Central Asia and western North America: positive PDO phases generally enhance rainfall in these regions, whereas negative phases suppress it [19]. The North Atlantic Oscillation (NAO) primarily affects rainfall variability across the North Africa–Mediterranean sector by modulating the meridional displacement of the westerly jet, thereby altering the position of rain belts at the Sahara margin. Positive NAO phases strengthen and shift the westerlies northward, leading to reduced rainfall in North Africa, while negative phases favor deeper Mediterranean troughs and increased precipitation along the Saharan fringe. Collectively, these natural oscillations, intertwined with anthropogenic warming, produce complex “trend + cycle” interactions that shape the hydroclimate of drylands.

In addition to climatic drivers, human activities exert profound influences on hydrological processes in drylands. Large-scale irrigation and hydraulic engineering have substantially altered land–surface water cycling. Irrigation withdraws groundwater and river water for cropland, which on the one hand increases evapotranspiration and modifies local humidity and energy balance [46], but on the other hand reduces downstream runoff and groundwater storage, potentially causing river flow interruptions and declining water tables. Land-use change is another key factor. Overgrazing and vegetation degradation reduce soil moisture-holding capacity, intensify surface runoff and soil erosion, and make flood generation and rapid soil-water loss more likely during rainfall events [47]. In contrast, afforestation in some regions can enhance soil moisture retention and partly mitigate drought impacts [48]. Although urbanization and land sealing are relatively limited in drylands, they increase runoff coefficients locally, causing a higher fraction of precipitation to become surface runoff rather than infiltrating into the soil, a phenomenon observed in some oasis cities of the Middle East. Inter-basin water transfer projects also reshape the geographical distribution of water resources. For example, China’s South-to-North Water Transfer Project has alleviated groundwater depletion in the North China Plain to some extent, while simultaneously altering the water cycle in donor regions. These anthropogenic activities often interact with climate change: global warming alters the overall availability of water, whereas human use determines its redistribution across space and time. Current studies emphasize that the causes of aridification in drylands are multifactorial, involving not only climate warming but also soaring water demand from population growth and economic development, industrial activities such as oil extraction, large-scale hydraulic projects, land reclamation and abandonment, frequent wildfires, and overgrazing. Overall, human activities have become an indispensable factor shaping the water cycle in drylands. Their mechanisms are complex and diverse, and must be considered jointly with climatic influences.

5. Vegetation Responses to Hydrological Variables in Drylands

Precipitation is the principal water source for agriculture in drylands, and its amount and spatiotemporal distribution directly determine water availability during the growing season [49]. Using AVHRR NDVI and ERA5 precipitation datasets, this study quantified the relationship between vegetation and rainfall from 2001 to 2020 with Pearson correlation analysis (Figure 14a). Strong positive correlations (0.5 to 0.95) were observed in regions such as South America, central Africa, India, Southeast Asia, and inland Australia, indicating that NDVI increases significantly with rainfall, reflecting the ecological process of precipitation-driven vegetation growth. Precipitation is also a key determinant of crop yield. NeSmith and Ritchie highlighted that water availability has the greatest meteorological influence on crop productivity; for maize, for example, soil drought during flowering is particularly damaging and can cause substantial yield loss [50]. Unstable rainfall variability likewise undermines yield, with irregular precipitation fluctuations associated with sustained declines in maize production. In areas prone to seasonal drought, rainfall deficits during critical growth stages inhibit crop development and reproduction, leading to leaf wilting, floral sterility, and ultimately reduced yields or even crop failure [51]. Overall, rainfall deficiency is the direct trigger of agricultural drought in drylands, and its impact depends on both timing and magnitude. Early-season drought may suppress seedling establishment, whereas mid-to-late-season drought exerts the most severe impact on yield. Extreme precipitation events also affect dryland agriculture: heavy storms often generate surface runoff and soil erosion, preventing infiltration of valuable rainfall and limiting soil moisture replenishment, while floods may damage crops directly [52,53]. Thus, improving the efficiency of rainfall utilization is critical for sustaining crop growth in drylands.

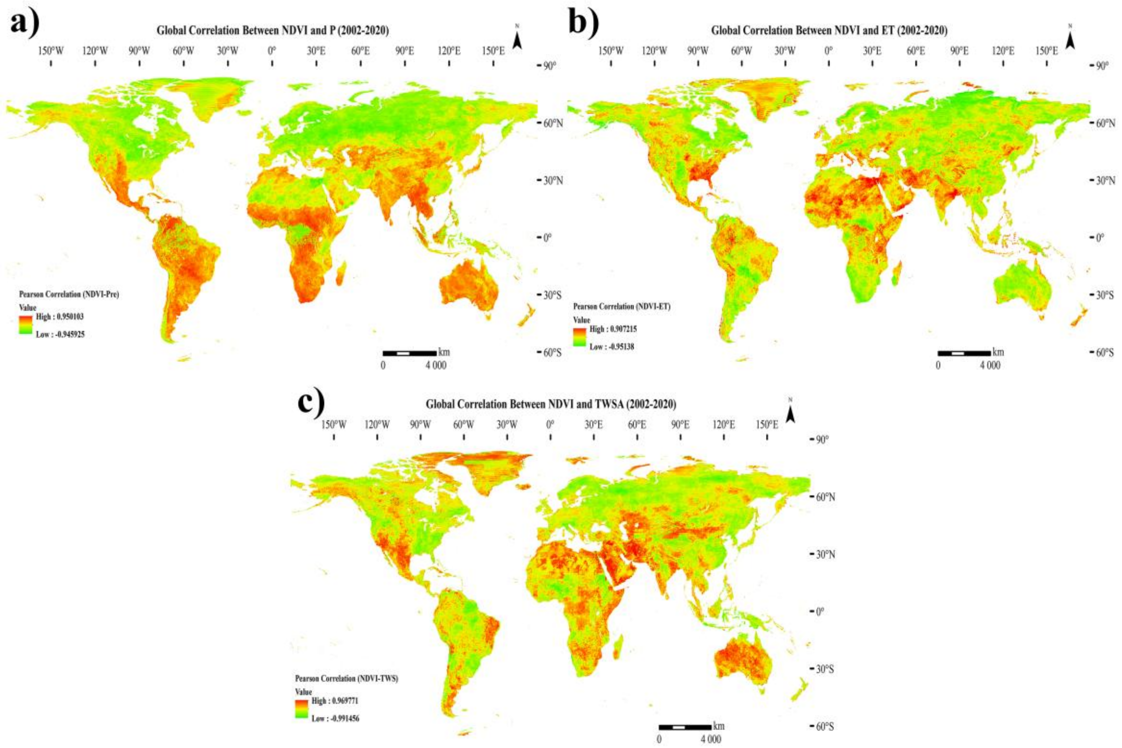

Figure 14. (**a**) Pearson correlation coefficients between NDVI and precipitation (P); (**b**) Pearson correlation coefficients between NDVI and evapotranspiration (ET); (**c**) Pearson correlation coefficients between NDVI and terrestrial water storage anomalies (TWSA).

Using AVHRR NDVI and ERA5 ET datasets, this study quantified the relationship between vegetation and evapotranspiration during 2001–2020 with Pearson correlation analysis (Figure 14b). Globally, NDVI and ET show strong positive correlations in tropical and temperate regions, particularly in South America, Southeast Asia, and Central Africa. In contrast, correlations weaken markedly—or even become negative—in drylands such as North Africa, West Asia, and central Australia, reflecting a "decoupling" between vegetation activity and evapotranspiration under water-limited conditions. Drylands are typically characterized by ample solar radiation, high temperatures, and low atmospheric humidity, resulting in high potential evapotranspiration. This substantially increases crop water demand, and if soil moisture supply cannot keep pace, water deficits emerge. With global warming, atmospheric aridity and evaporative demand are further intensified, aggravating imbalances in cropland water budgets. Martínez-Vilalta and Garcia-Forner showed that in hot, arid environments, when ET greatly exceeds precipitation inputs, crops are highly susceptible to water stress and often reduce transpiration as a protective mechanism [54]. However, while stomatal closure limits water loss, it also restricts CO_2 uptake and photosynthesis, ultimately suppressing biomass accumulation and yield [55]. ET dynamics are also influenced by crop type and growth stage: during late growth stages, when canopy closure and leaf area index are high, ET is elevated, whereas croplands at seedling stage or fallow periods exhibit lower ET [56,57]. Therefore, irrigation in drylands should be scheduled in accordance with stage-specific ET patterns to prevent severe water deficits during critical phases of crop development.

Runoff refers to the portion of precipitation that flows over the land surface. In drylands, rainfall is often intense but short in duration, and infiltration rates are low due to dry or compacted surface soils. As a result, rainfall readily transforms into surface runoff. Excessive runoff not only prevents effective storage of precipitation as soil moisture but also accelerates soil erosion, washing away topsoil nutrients and further weakening soil moisture- and nutrient-retention capacity [58]. Consequently, runoff processes reduce the already limited efficiency of rainfall utilization in drylands—particularly on sloping land and sandy soils—where fields often dry rapidly after heavy rain, leaving crops unable to make full use of the water. By contrast, flat terrain or farmland equipped with water-harvesting infrastructure can intercept part of the runoff, converting it into useful soil moisture or groundwater recharge. Overall, reducing ineffective runoff losses and enhancing rainfall infiltration are critical strategies for agriculture in drylands [59]. For example, Yu, et al. demonstrated that surface mulching can reduce raindrop splash and runoff while improving soil moisture storage [60]. Through engineering interventions and farm management practices, enabling more precipitation to infiltrate rather than run off is key to conserving soil moisture and improving yields in dryland agriculture.

Soil moisture represents the form of moisture directly available for crop root uptake and serves as a critical intermediary linking precipitation, irrigation, and crop growth. Crop development is highly sensitive to soil moisture content: when soil moisture is deficient, plants exhibit smaller leaves, restricted stem elongation, and slower root growth, with a concurrent decline in water-use efficiency [61]. Water stress–induced wilting suppresses photosynthesis and nutrient transport, while prolonged drought may cause irreversible growth stagnation and yield loss. Conversely, excessive soil moisture from heavy rainfall or improper irrigation can induce temporary waterlogging, displacing soil oxygen, damaging root systems, and resulting in poor growth or yield reductions [62]. Thus, soil moisture availability is optimal within a specific range—below field capacity but above the permanent wilting point. Water closer to the wilting point is difficult for roots to absorb and therefore less effective, whereas moisture nearer to field capacity is more easily accessible and effective for plant use. In drylands, soil moisture shows strong spatial and temporal variability: surface layers dry rapidly, while deeper layers, if previously recharged, can sustain crops during mid- to late-season droughts. For this reason, drought-tolerant crops such as wheat and cotton extend their roots deeper into the soil profile to access subsurface water reserves. Shoaib, et al. demonstrated that increasing soil organic matter enhances soil moisture-holding capacity and improves crop drought resistance [63]. Overall, maintaining stable soil moisture supply and avoiding extended dry periods are fundamental requirements for normal crop growth. In agricultural practice, soil moisture is regulated through monitoring, appropriate irrigation, and mulching techniques to buffer the impacts of drought on crops.

Groundwater is a vital water reserve in drylands, and its depth and dynamic fluctuations strongly influence water availability for crops. Because terrestrial water storage anomalies (TWSA) in drylands are largely governed by groundwater storage anomalies (GWSA) [64–67], we used AVHRR NDVI and GRACE TWSA datasets to quantify their correlation globally from 2002 to 2020 (Figure 14c). In dryland regions such as Central Asia, the Iranian Plateau, North Africa, inland Australia, and the southwestern United States, NDVI and TWSA exhibit strong positive correlations, indicating that groundwater fluctuations exert substantial regulatory effects on vegetation ecosystems. This relationship is especially pronounced in areas with minimal precipitation, where groundwater serves as a critical sustaining source for vegetation cover. By contrast, in humid zones such as equatorial rainforests, the South Asian monsoon belt, and much of Europe, the correlations are weak or absent, with vegetation growth relying primarily on soil moisture or direct precipitation. In some areas, however—such as northern India and the middle–lower Yellow River Plain—negative correlations are observed, likely reflecting the impacts of groundwater overextraction that induces soil desiccation, land subsidence, or crop stress, thereby underscoring the complex human disturbances to water–vegetation interactions. For deep-rooted crops, shallow water tables may provide supplementary benefits during drought, as root systems can access groundwater through capillary rise [68]. In the U.S. Corn Belt, Deines et al. found that when groundwater tables were within a "recharge window" of ~1.1–2.5 m, maize yields increased by an average of 3.4% relative to areas without groundwater support, and yield gains doubled during drought years [68]. Conversely, excessively deep water tables preclude root access, while shallow water tables (<1 m) may cause waterlogging or secondary salinization, both of which negatively affect crop growth. Crop sensitivity to groundwater depth also varies by species. Fawen, et al. demonstrated that wheat can effectively utilize groundwater when the water table is ~1 m, whereas cotton is more sensitive to water-table depth, requiring an optimal range to realize yield benefits [69]. This suggests that cotton is vulnerable both to waterlogging from shallow water tables and to limited access under deeper conditions [70]. In many irrigated dryland regions, groundwater accessed through pumping is the primary water source for agriculture. Yet overexploitation continues to lower water tables, undermining the long-term drought-buffering capacity of aquifers. Consequently, sustainable groundwater use and management are essential, including regulating abstraction to maintain water tables within suitable depths and integrating surface irrigation with rainfall infiltration to enhance recharge.

In summary, each hydrological variable exerts a significant influence on plant growth: precipitation provides the direct water supply; evapotranspiration reflects atmospheric water demand; runoff governs infiltration and storage; soil moisture represents the accessible water for roots; and groundwater serves as a deeper buffer source. Under arid conditions, these components are interlinked and jointly determine the overall water status experienced by vegetation. It should be noted that, due to NDVI and hydrological variables are spatially continuous, the pixel-wise correlations presented in Figure 14 are influenced by spatial autocorrelation, which may inflate apparent significance. Therefore, these correlations should be regarded as descriptive indicators of large-scale spatial co-variation rather than statistically independent tests.

6. Discussion

This review has synthesized the changes in key hydrological variables in drylands, including precipitation, evapotranspiration, soil moisture, and groundwater, and examined their spatiotemporal evolution and driving mechanisms. Advances in remote sensing satellite technology have greatly improved scientific understanding of water cycle processes in drylands. Nevertheless, from the perspective of data consistency, discrepancies remain among different sources—including satellite observations, model simulations, and gravity-based inversions—in describing hydrological changes in drylands. Such inconsistencies introduce substantial uncertainty into the assessment of water resources in these regions.

From a methodological perspective, remote sensing and reanalysis data have greatly extended the spatial and temporal scales at which hydrological processes in drylands can be monitored. High-frequency satellite products provide extensive surface information, making drought monitoring feasible even in regions where traditional observations are sparse. Nonetheless, satellite observations remain constrained by cloud contamination, limited resolution, and retrieval uncertainties, with accuracy challenges particularly evident in drylands characterized by complex topography and strong surface heterogeneity. Similarly, while reanalysis datasets offer physical consistency and long-term continuity, they still have limitations in capturing human activities, land-use changes, and local microclimatic effects. A critical future direction is therefore to develop more effective frameworks for integrating satellite observations, in situ measurements, and model outputs to build more robust and accurate hydrological datasets, thereby providing reliable support for water resource management in drylands.

Long-term trend analyses have shown that in many dryland regions worldwide, evapotranspiration has continued to increase, even in the absence of significant precipitation growth. This imbalance—where evaporation outpaces rainfall—has intensified water deficits, driven soil drying, and heightened the risk of crop water stress. Rising evapotranspiration not only reflects increasing vegetation water demand but also shortens the duration of soil water availability, thereby raising the frequency of water shortages during the growing season. Under a climate regime marked by high rainfall variability and more frequent extreme heat events, this trend already poses a substantial threat to dryland vegetation. At the same time, dependence on groundwater in drylands continues to rise. Globally, about 70% of groundwater withdrawals are for agricultural use, and this proportion is even higher in drylands [71]. However, observations from multiple regions reveal that overexploitation is driving sustained declines in groundwater levels, severely undermining both the sustainability of agricultural water supply and the stability of ecosystems [72].

Although precipitation and vegetation are closely linked, their relationship is not instantaneous. Vegetation often responds to rainfall with a delay ranging from several weeks to a few months, depending on soil moisture retention, rooting depth, and plant physiological adjustment. This lag effect means that vegetation greenness can remain high for a short period after rainfall ceases or decline even when precipitation temporarily increases. In long-term trend analyses, annual aggregation tends to smooth these short-term fluctuations, capturing the overall co-variation between vegetation and hydrological variables rather than the precise timing of their responses.

Therefore, the results presented here should be interpreted as indicative of large-scale coupling patterns rather than immediate cause-and-effect dynamics.

Future sustainable development in drylands requires systematic modeling of coupled hydrology–vegetation systems. Most existing studies remain focused on correlations among variables, with limited exploration of the internal feedback mechanisms linking climate, hydrology, and vegetation. Future research should therefore emphasize the construction and integration of process-based models—for example, coupling meteorological, hydrological, and vegetation models—to identify response thresholds and nonlinear effects of vegetation systems under different hydrological change scenarios. In addition, causal analysis tools such as structural equation modeling and lagged causal networks should be applied to uncover potential driving pathways among variables and to avoid misinterpreting mechanisms based solely on temporal coincidence. Recent studies indicate that shallow groundwater provides an important form of "hidden irrigation" for crop growth: when the water table is maintained at certain depths, crop yields can increase substantially during drought years; by contrast, deeper water tables lose their buffering capacity and may even constrain root water uptake. This further underscores the necessity of incorporating groundwater–crop interactions into integrated hydrology–vegetation modeling frameworks.

7. Future Prospects and Challenges

(1) Partitioning dryland hydrological components for groundwater protection: Future research should prioritize quantifying how each component of the hydrological cycle in drylands contributes to the water balance—specifically, how limited precipitation is partitioned into evapotranspiration, soil moisture, runoff, and groundwater recharge. This focus is crucial because in many dryland regions over 90% of rainfall can be lost to evapotranspiration, with less than 1% generating surface runoff and only a small fraction percolating to aquifers [73]. A better understanding of these partitions will help identify strategies to enhance groundwater replenishment, and reduce unnecessary water losses. High-resolution monitoring and modeling tailored to dryland conditions are needed to capture processes like brief high-intensity rains, transmission losses, and focused infiltration, which are often overlooked in generic models. By improving the accuracy of water-balance estimation in drylands, researchers can provide actionable guidance to protect vulnerable aquifers and sustain terrestrial water storage under the twin pressures of climate stress and overextraction.

(2) Managing extreme climate swings to boost dryland resilience: As climate variability intensifies, drylands will more frequently face compound extreme events, such as rapid shifts from prolonged drought to intense rainfall. These whiplash events can overwhelm dryland hydrology and agriculture, causing flash floods, soil erosion, and nutrient losses, for instance, a single drought–flood sequence can reduce soil nitrogen storage by ~15% while increasing nutrient runoff by over 50% [74–76]. Future studies should systematically assess the nonlinear and cumulative impacts of such extremes on watershed processes, vegetation, and crop yields. Improving early-warning systems and predictive models for these abrupt drought–flood cycles is essential. Equally important is developing adaptation measures to help dryland societies absorb shocks, such as water diversion infrastructure, drought-tolerant crop varieties, and flexible grazing or irrigation schedules. By investigating how ecosystems respond to and recover from extreme-event sequences, researchers can inform policies and practices that strengthen the resilience of dryland regions in the face of climate extremes.

Overall, a more forward-looking and policy-driven approach is needed to safeguard dryland water security under changing conditions. All dryland regions worldwide would benefit from scientists and engineers collaborating with water managers and policymakers to translate these research insights into action. Every aspect of the dryland water cycle must be assessed and integrated into flexible management strategies. This includes implementing sustainable water conservation practices, robust groundwater governance, and climate adaptation policies that can adjust as conditions evolve. By coupling rigorous scientific research with proactive policy measures, we can ensure that dryland ecosystems and communities remain resilient and sustainable in the long term.

8. Conclusions

This study compared widely used remote sensing datasets from multiple perspectives and employed multi-source observations to analyze the spatiotemporal evolution of hydrological variables worldwide from 2001 to 2022, with a particular focus on precipitation, evapotranspiration, soil moisture, groundwater, and terrestrial water storage in drylands. The results show that during the study period, global precipitation increased significantly at a rate of 0.62 mm yr^{-1}, yet precipitation in drylands declined and their extent expanded. Global evapotranspiration rose significantly at 2.26 mm yr^{-1}, with high values concentrated in drylands. In contrast, groundwater storage declined at 2.18 mm yr^{-1}, with sharp reductions in several dryland regions. Terrestrial water storage decreased at 3.16 mm yr^{-1}, with widespread negative anomalies across drylands. Correlation analyses between NDVI and hydrological variables reveal that vegetation in drylands is generally positively related to precipitation, negatively associated with evapotranspiration, and positively linked to terrestrial water storage.

The evolution of hydrological processes in drylands is jointly driven by climate change, natural variability, and human activities. Global warming enhances atmospheric evaporative demand and alters circulation patterns, intensifying aridification. Large-scale climate oscillations such as ENSO, PDO, AMO, and NAO modulate interannual and decadal precipitation variability, which, combined with long-term warming, create complex "trend + cycle" dynamics. Human activities—including irrigation withdrawals, hydraulic projects, land-use change, and urbanization—reshape the spatial and temporal distribution of water and exacerbate resource imbalances. Overall, climate change defines the broader water budget, natural oscillations regulate variability, and human activities redistribute water resources, together driving the hydrological evolution of drylands.

This review provides a theoretical basis and research framework for future work on coupled hydrology–ecosystem modeling, multi-scale monitoring and assessment, and adaptation to climate extremes in drylands, with implications for optimizing regional water allocation and promoting ecological sustainability.

Author Contributions

J.X.: conceptualization, data curation, writing—original draft preparation; F.G.: supervision, methodology, writing—review and editing; L.J.: visualization, investigation; J.Z.: validation, resources; S.S.: funding acquisition, project administration; F.G.: resources, investigation; X.H.: supervision, funding acquisition, project administration; P.J.: funding acquisition, project administration. All authors have read and agreed to the published version of the manuscript.

Funding

This research was funded by the Major Science and Technology Project of Xinjiang Autonomous Region (2023A02002-1), Special project of scientific and technological innovation of Xinjiang Research Institute of Arid Area Agriculture (XJHQNY-3), National Natural Science Foundation of China (W2412160), Research Project of Shaanxi Laboratory for Arid Region Agriculture (2024ZY-JCYJ-02-40), Shanghai Cooperation Institute of Modern Agricultural Development (SCO24A001).

Institutional Review Board Statement

Not applicable.

Informed Consent Statement

Not applicable.

Data Availability Statement

Data will be made available on request.

Conflicts of Interest

The authors declare that they have no known competing financial interests or personal relationships that could have appeared to influence the work reported in this paper.

Use of AI and AI-Assisted Technologies

No AI tools were utilized for this paper.

References

1. Ambika, A.K.; Mishra, V. Substantial decline in atmospheric aridity due to irrigation in India. *Environ. Res. Lett.* **2020**, *15*, 124060.
2. An, L.; Wang, J.; Huang, J.; et al. Divergent Causes of Terrestrial Water Storage Decline Between Drylands and Humid Regions Globally. *Geophys. Res. Lett.* **2021**, *48*. https://doi.org/10.1029/2021gl095035.
3. Bayad, M.; Chau, H.W.; Trolove, S.; et al. Surface runoff and losses of phosphorus from hydrophobic pastoral soils. *Agric. Ecosyst. Environ.* **2022**, *324*, 107690. https://doi.org/10.1016/j.agee.2021.107690.
4. Beyer, M.; Wallner, M.; Bahlmann, L.; et al. Rainfall characteristics and their implications for rain-fed agriculture: A case study in the Upper Zambezi River Basin. *Hydrol. Sci. J.* **2016**, *61*, 321–343.

5. Bhattacharya, A. Effect of Soil Water Deficit on Growth and Development of Plants: A Review. In *Soil Water Deficit and Physiological Issues in Plants*; Springer: Heidelberg, Germany, 2021; pp. 393–488. https://doi.org/10.1007/978-981-33-6276-5_5.
6. Bi, W.; Hu, Y.; Weng, B.; et al. Drought–flood abrupt alternation events increase soil nitrogen loss via surface runoff in a typical grain base in China. *J. Hydrol. Reg. Stud.* **2025**, *60*, 102543. https://doi.org/10.1016/j.ejrh.2025.102543.
7. Bi, W.; Weng, B.; Yan, D.; et al. Soil phosphorus loss increases under drought-flood abrupt alternation in summer maize planting area. *Agric. Water Manag.* **2022**, *262*, 107426. https://doi.org/10.1016/j.agwat.2021.107426.
8. Lin, C.; Bie, Q.; Yao, W. *Global Classification of Arid Zones (1970–2020)*; National Tibetan Plateau Data Center: Beijing, China, 2025. https://doi.org/10.11888/Terre.tpdc.302120.
9. Chang, L.L.; Yuan, R.; Gupta, H.V.; et al. Why Is the Terrestrial Water Storage in Dryland Regions Declining? A Perspective Based on Gravity Recovery and Climate Experiment Satellite Observations and Noah Land Surface Model With Multiparameterization Schemes Model Simulations. *Water Resour. Res.* **2020**, *56*. https://doi.org/10.1029/2020wr027102.
10. Chawla, I.; Karthikeyan, L.; Mishra, A.K. A review of remote sensing applications for water security: Quantity, quality, and extremes. *J. Hydrol.* **2020**, *585*, 124826. https://doi.org/10.1016/j.jhydrol.2020.124826.
11. Chemke, R. The future poleward shift of Southern Hemisphere summer mid-latitude storm tracks stems from ocean coupling. *Nat. Commun.* **2022**, *13*, 1730. https://doi.org/10.1038/s41467-022-29392-4.
12. Chen, L.; Liu, L.; Liu, S.; et al. The Application of Remote Sensing Technology in Inland Water Quality Monitoring and Water Environment Science: Recent Progress and Perspectives. *Remote Sens.* **2025**, *17*, 667.
13. Cheng, Y.; Zhang, X.; Wang, K.; et al. Multidimensional evaluation of satellite-based and reanalysis-based precipitation datasets in the Tibetan Plateau. *J. Hydrol.* **2025**, *660*, 133364. https://doi.org/10.1016/j.jhydrol.2025.133364.
14. Claassen, M.; Shaw, R.H. Water deficit effects on corn. II. Grain components 1. *Agron. J.* **1970**, *62*, 652–655.
15. Cui, J.; Lian, X.; Huntingford, C.; et al. Global water availability boosted by vegetation-driven changes in atmospheric moisture transport. *Nat. Geosci.* **2022**, *15*, 982–988. https://doi.org/10.1038/s41561-022-01061-7.
16. Deines, J.; Archontoulis, S.; Huber, I.; et al. Observational evidence for groundwater influence on crop yields in the United States. *Proc. Natl. Acad. Sci. USA* **2024**, *121*, e2400085121. https://doi.org/10.1073/pnas.2400085121.
17. Demo, A.H.; Asefa Bogale, G. Enhancing crop yield and conserving soil moisture through mulching practices in dryland agriculture. *Front. Agron.* **2024**, *6*, 1361697.
18. Fawen, L.; Yutong, L.; Jun, F. Effect of the groundwater fluctuation process on crop growth in Shijin irrigation district. *Water Policy* **2022**, *24*, 1394–1413. https://doi.org/10.2166/wp.2022.249.
19. Feng, H.; Zhang, M. Global land moisture trends: Drier in dry and wetter in wet over land. *Sci. Rep.* **2015**, *5*, 18018. https://doi.org/10.1038/srep18018.
20. Folland, C.K.; Palmer, T.N.; Parker, D.E. Sahel rainfall and worldwide sea temperatures, 1901–1985. *Nature* **1986**, *320*, 602–607.
21. Francis, D.; Fonseca, R. Recent and projected changes in climate patterns in the Middle East and North Africa (MENA) region. *Sci. Rep.* **2024**, *14*, 10279. https://doi.org/10.1038/s41598-024-60976-w.
22. Giannini, A.; Saravanan, R.; Chang, P. Oceanic forcing of Sahel rainfall on interannual to interdecadal time scales. *Science* **2003**, *302*, 1027–1030.
23. Giardina, F.; Gentine, P.; Konings, A.G.; et al. Diagnosing evapotranspiration responses to water deficit across biomes using deep learning. *New Phytol.* **2023**, *240*, 968–983. https://doi.org/10.1111/nph.19197.
24. Girotto, M.; Rodell, M. Terrestrial Water Storage. In *Extreme Hydroclimatic Events and Multivariate Hazards in a Changing Environment*; Elsevier: Amsterdam, The Netherlands, 2019; pp. 41–64.
25. Government of Australia. *State of the Climate*; Government of Australia: Canberra, Australia, 2024.
26. Hssaisoune, M.; Bouchaou, L.; Sifeddine, A.; et al. Moroccan Groundwater Resources and Evolution with Global Climate Changes. *Geosciences* **2020**, *10*, 81.
27. Hu, Z.; Zhou, Q.; Chen, X.; et al. Groundwater Depletion Estimated from GRACE: A Challenge of Sustainable Development in an Arid Region of Central Asia. *Remote Sens.* **2019**, *11*, 1908.
28. IPCC. Climate Change 2021: The Physical Science Basis. In *Contribution of Working Group I to ,the Sixth Assessment Report of the Intergovernmental Panel on Climate Change*; Masson-Delmotte, V., Zhai, P., Pirani, A., et al., Eds.; Cambridge University Press: Cambridge, UK, 2021; pp. 2215–2256. https://doi.org/10.1017/9781009157896.022.
29. Jasechko, S.; Seybold, H.; Perrone, D.; et al. Rapid groundwater decline and some cases of recovery in aquifers globally. *Nature* **2024**, *625*, 715–721. https://doi.org/10.1038/s41586-023-06879-8.
30. Jin, X.; Kumar, L.; Li, Z.; et al. A review of data assimilation of remote sensing and crop models. *Eur. J. Agron.* **2018**, *92*, 141–152. https://doi.org/10.1016/j.eja.2017.11.002.
31. Jung, M.; Reichstein, M.; Ciais, P.; et al. Recent decline in the global land evapotranspiration trend due to limited moisture supply. *Nature* **2010**, *467*, 951–954.

32. Kasampalis, D.A.; Alexandridis, T.K.; Deva, C.; et al. Contribution of Remote Sensing on Crop Models: A Review. *J. Imaging* **2018**, *4*, 52.
33. Kou, P.; Xu, Q.; Jin, Z.; et al. Analyzing gully erosion and deposition patterns in loess tableland: Insights from small baseline subset interferometric synthetic aperture radar (SBAS InSAR). *Sci. Total Environ.* **2024**, *916*, 169873. https://doi.org/10.1016/j.scitotenv.2024.169873.
34. Kou, P.; Xu, Q.; Jin, Z.; et al. Rill erosion on an unpaved loess road surface: Effects and control. *Land Degrad. Dev.* **2023**, *34*, 1752–1766. https://doi.org/10.1002/ldr.4566.
35. Kou, P.; Xu, Q.; Jin, Z.; et al. Complex anthropogenic interaction on vegetation greening in the Chinese Loess Plateau. *Sci. Total Environ.* **2021**, *778*, 146065. https://doi.org/10.1016/j.scitotenv.2021.146065.
36. Kou, P.; Xu, Q.; Yunus, A.P.; et al. Micro-topographic assessment of rill morphology highlights the shortcomings of current protective measures in loess landscapes. *Sci. Total Environ.* **2020**, *737*, 139721. https://doi.org/10.1016/j.scitotenv.2020.139721.
37. Kou, P.; Xu, Q.; Yunus, A.P.; et al. Rill development and its change rate: A field experiment under constant rainfall intensity. *Catena* **2021**, *199*, 105112. https://doi.org/10.1016/j.catena.2020.105112.
38. Li, Z.; Zhang, Z.; Zhang, L. Improving regional wheat drought risk assessment for insurance application by integrating scenario-driven crop model, machine learning, and satellite data. *Agric. Syst.* **2021**, *191*, 103141. https://doi.org/10.1016/j.agsy.2021.103141.
39. Liu, G.; Wang, W. Competing effects of vegetation greening-induced changes in summer evapotranspiration and precipitation on water yield in the Yangtze River Basin based on WRF simulations. *Water Resour. Res.* 2025, 61, e2024WR038663.
40. Liu, X.; Feng, X.; Ciais, P.; et al. Widespread decline in terrestrial water storage and its link to teleconnections across Asia and eastern Europe. *Hydrol. Earth Syst. Sci.* **2020**, *24*, 3663–3676. https://doi.org/10.5194/hess-24-3663-2020.
41. Liu, X.; Peng, X.; Li, Y.; et al. Environmental influences on evapotranspiration in wheat-maize rotation systems under diverse hydrological regimes in the Guanzhong Plain, China. *Agric. Water Manag.* **2024**, *306*, 109204. https://doi.org/10.1016/j.agwat.2024.109204.
42. Luo, M.; Liu, Y.; Luo, R.; et al. Anthropogenic Impacts on the Water Cycle over Drylands in the Northern Hemisphere. *J. Clim.* **2023**, *36*, 453–466. https://doi.org/10.1175/JCLI-D-22-0037.1.
43. Maina, F.Z.; Kumar, S.V.; Albergel, C.; et al. Warming, increase in precipitation, and irrigation enhance greening in High Mountain Asia. *Commun. Earth Environ.* **2022**, *3*, 43. https://doi.org/10.1038/s43247-022-00374-0.
44. Martínez-Vilalta, J.; Garcia-Forner, N. Water potential regulation, stomatal behaviour and hydraulic transport under drought: Deconstructing the iso/anisohydric concept. *Plant Cell Environ.* **2017**, *40*, 962–976.
45. McCabe, G.J.; Palecki, M.A.; Betancourt, J.L. Pacific and Atlantic Ocean influences on multidecadal drought frequency in the United States. *Proc. Natl. Acad.Sci. USA* **2004**, *101*, 4136–4141.
46. Meixner, T.; Manning, A.H.; Stonestrom, D.A.; et al. Implications of projected climate change for groundwater recharge in the western United States. *J. Hydrol.* **2016**, *534*, 124–138. https://doi.org/10.1016/j.jhydrol.2015.12.027.
47. Ndehedehe, C.E.; Adeyeri, O.E. Changes in Drought Characteristics and Heatwave Propagation Over Groundwater Basins in Australia. *Earth Syst. Environ.* **2024**, 1-20. https://doi.org/10.1007/s41748-024-00463-4.
48. NeSmith, D.; Ritchie, J. Effects of soil water-deficits during tassel emergence on development and yield component of maize (*Zea mays*). *Field Crops Res.* **1992**, *28*, 251–256.
49. Park, J.; Bader, J.; Matei, D. Anthropogenic Mediterranean warming essential driver for present and future Sahel rainfall. *Nat. Clim. Change* **2016**, *6*, 941–945. https://doi.org/10.1038/nclimate3065.
50. Quichimbo, E.A.; Singer, M.B.; Michaelides, K.; et al. DRYP 1.0: A parsimonious hydrological model of DRYland Partitioning of the water balance. *Geosci. Model Dev.* **2021**, *14*, 6893–6917. https://doi.org/10.5194/gmd-14-6893-2021.
51. Ramezani Etedali, H.; Gorginpaveh, F.; Elbeltagi, A.; et al. Estimation of actual evapotranspiration and water requirements of strategic crops under different stresses. *Sci. Rep.* **2025**, *15*, 7778. https://doi.org/10.1038/s41598-025-92481-z.
52. Sardans, J.; Miralles, A.; Tariq, A.; et al. Growing aridity poses threats to global land surface. *Commun. Earth Environ.* **2024**, *5*, 776. https://doi.org/10.1038/s43247-024-01935-1.
53. Scanlon, B.R.; Faunt, C.C.; Longuevergne, L.; et al. Groundwater depletion and sustainability of irrigation in the US High Plains and Central Valley. *Proc. Natl. Acad. Sci. USA* **2012**, *109*, 9320–9325. https://doi.org/10.1073/pnas.1200311109.
54. Seo, K.W.; Ryu, D.; Jeon, T.; et al. Abrupt sea level rise and Earth's gradual pole shift reveal permanent hydrological regime changes in the 21st century. *Science* **2025**, *387*, 1408–1413. https://doi.org/10.1126/science.adq6529.
55. Sharma, R.K.; Kumar, S.; Vatta, K.; et al. Impact of recent climate change on corn, rice, and wheat in southeastern USA. *Sci. Rep.* **2022**, *12*, 16928. https://doi.org/10.1038/s41598-022-21454-3.
56. Shoaib, M.; Banerjee, B.P.; Hayden, M.; et al. Roots' drought adaptive traits in crop improvement. *Plants* **2022**, *11*, 2256.
57. Singh, N.K.; Saia, S.M.; Bhattacharya, R.; et al. Unraveling the causal influences of drought and crop production on groundwater levels across the contiguous United States. *PNAS Nexus* **2025**, *4*, pgaf129. https://doi.org/10.1093/pnasnexus/pgaf129.
58. Sutton, R.T.; Hodson, D.L. Climate response to basin-scale warming and cooling of the North Atlantic Ocean. *J. Clim.* **2007**, *20*, 891–907.

59. Tamarin-Brodsky, T.; Kaspi, Y. Enhanced poleward propagation of storms under climate change. *Nat. Geosci.* **2017**, *10*, 908–913.
60. Tariq, A.; Graciano, C.; Sardans, J.; et al. Decade-long unsustainable vegetation management practices increase macronutrient losses from the plant-soil system in the Taklamakan Desert. *Ecol. Indic.* **2022**, *145*, 109653.
61. Todd Jarvis, W. Groundwater Around the World: A Geographic Synopsis. *Ground Water* **2013**, *51*, 486.
62. UNEP. *World Atlas of Desertification*; UNEP: Nairobi, Kenya, 1992.
63. UNESCO. *United Nations World Water Development Report 2022: Groundwater: Making the Invisible Visible*; UNESCO: Paris, France, 2022.
64. Urrego, J.P.F.; Huang, B.; Næss, J.S.; et al. Meta-analysis of leaf area index, canopy height and root depth of three bioenergy crops and their effects on land surface modeling. *Agric. For. Meteorol.* **2021**, *306*, 108444. https://doi.org/10.1016/j.agrformet.2021.108444.
65. Vizy, E.K.; Cook, K.H. Mechanisms by which Gulf of Guinea and eastern North Atlantic sea surface temperature anomalies can influence African rainfall. *J. Clim.* **2001**, *14*, 795–821.
66. Walker, G.R.; Crosbie, R.S.; Chiew, F.H.S.; et al. Groundwater Impacts and Management under a Drying Climate in Southern Australia. *Water* **2021**, *13*, 3588.
67. Wang, C.; Li, S.; Kang, S.; et al. Evapotranspiration and potential water saving effect evaluation of mulched maize fields in China. *J. Hydrol.* **2024**, *630*, 130658. https://doi.org/10.1016/j.jhydrol.2024.130658.
68. Xu, B.; Yang, Q.; Ma, Z. Decadal characteristics of global land annual precipitation variation on multiple spatial scales. *Chin. J. Atmos. Sci.* **2017**, *41*, 593–602.
69. Yan, X.; Cheng, P.; Zhang, Q.; et al. Comparisons of climate change characteristics in typical arid regions of the Northern Hemisphere. *Front. Environ. Sci.* **2022**, *10*, 1033326.
70. Yan, X.; Cheng, P.; Zhang, Q.; et al. Progress in joint application of crop models and hydrological models. *Agric. Water Manag.* **2024**, *295*, 108746. https://doi.org/10.1016/j.agwat.2024.108746.
71. Yu, Y.Y.; Turner, N.C.; Gong, Y.H.; et al. Benefits and limitations to straw-and plastic-film mulch on maize yield and water use efficiency: A meta-analysis across hydrothermal gradients. *Eur. J. Agron.* **2018**, *99*, 138–147.
72. Yuan, X.; Wang, W.; Cui, J.; et al. Vegetation changes and land surface feedbacks drive shifts in local temperatures over Central Asia. *Sci. Rep.* **2017**, *7*, 3287. https://doi.org/10.1038/s41598-017-03432-2.
73. Zhang, G.; Xu, T.; Yin, W.; et al. A machine learning downscaling framework based on a physically constrained sliding window technique for improving resolution of global water storage anomaly. *Remote Sens. Environ.* **2024**, *313*, 114359. https://doi.org/10.1016/j.rse.2024.114359.
74. Zhang, Y.; Zhang, Y.; Lian, X.; et al. Enhanced dominance of soil moisture stress on vegetation growth in Eurasian drylands. *Natl. Sci. Rev.* 2023, 10, nwad108. https://doi.org/10.1093/nsr/nwad108.
75. Zhao, M.; A, G.; Zhang, J.; et al. Ecological restoration impact on total terrestrial water storage. *Nat. Sustain.* **2020**, *4*, 56–62. https://doi.org/10.1038/s41893-020-00600-7.
76. Zhao, M.; McCormick, E.L.; A, G.; et al. Substantial root-zone water storage capacity observed by GRACE and GRACE/FO. *Hydrol. Earth Syst. Sci.* **2025**, *29*, 2293–2307. https://doi.org/10.5194/hess-29-2293-2025.